ABSTRACT

Title of thesis: WLAN SIGNAL CHARACTERISTICS IN AN INDOOR ENVIRONMENT – AN ANALYTIC MODEL AND EXPERIMENTS

Damayanti Gupta, Master of Science, 2005

Thesis directed by: Professor Ashok Agrawala,
Department of Computer Science

In today's environment, in which WLAN technology is being deployed extensively, in order to improve the effectiveness of such deployments it is necessary to have a detailed understanding of WLAN signal characteristics. Radio signal attenuation and path losses depend on the environment and have been recognized to be difficult to calculate and predict. Past studies of the signal propagation, in both an indoor and in an outdoor environment have used several models with varying degrees of success and/ or complexity. I present here a simple analytic model for an indoor environment, and use it for determining the signal strength in a 3-D environment with one transmitter. The model is experimentally verified and is shown to yield a good match with the measurements. Several consequences of the model are studied and contour plots mapping signal strengths are generated. Signal strengths in the presence of an obstruction in the field of the transmitter are studied.

WLAN SIGNAL CHARACTERISTICS IN AN INDOOR ENVIRONMENT - AN ANALYTIC MODEL AND EXPERIMENTS

by

Damayanti Gupta

Thesis submitted to the Faculty of the Graduate School of the
University of Maryland, College Park in partial fulfillment
of the requirements for the degree of
Master of Science
2005

Advisory Committee:
Prof. Ashok K. Agrawala, Chair
Dr Samrat Bhattacharjee
Dr. Amitabh Varshney

Acknowledgements

I would like to acknowledge significant help provided by Ms Rashi Narain, in conducting the experiments.

Table of Contents

Chapter 1. Introduction

1.1 Motivation

Wireless LAN technology, in particular 802.11b and 802.11g technology, has been gaining prominence in its use and deployment. In this technology, wireless communication in the 2.4 GHz band is used for digital communication at the rates of 11 Mbps for 802.11b and up to 54 Mbps for 802.11g. The current technology supports access to the wireless network through the deployment of Access Points (APs), which can be accessed within a radius of a few hundred feet (both indoors and outdoors). The range and the quality of the connection depend on the environment, the walls, and other obstructions, reflecting surfaces, etc., that are there in the path from the transmitter to the receiver. In order to not only improve the digital communication in such environments, but also to use the availability of these signals for other purposes such as determining locations, we need to understand the signal characteristics in detail. In this thesis I present the results of one such study in which I use an analytic model of signal propagation to determine signal strength at various locations in a 3-D region in the shape of a rectangular box. The models used in this study were empirically verified by making signal strength measurements.

The study presented here is part of a larger project which is aimed at exploiting the detailed knowledge of the signal characteristics to better manage WiFi deployments and in improving the quality of digital communications in such environments.

1.2 My Work

RF signal propagation follows well known laws of physics. An RF wave emitted by an antenna is attenuated due to distance in a direct line of sight (LoS) path. Also, the receiver may receive multiple such waves in an indoor environment due to reflection and other such phenomena [15]. The signal strength at the receiver depends on all such component waves; their amplitudes as well as their phases. In this study I take a simplistic view, taking into account the direct LoS signal, and signals received after a single reflection off of each of the available walls. I consider a rectangular box corresponding to a corridor in a building and develop an analytic model of the signal strength at various locations in this region when one transmitting antenna is deployed at a specified location. For verification of the model I measured the actual signal strengths in a corridor in the A.V. Williams building, University of Maryland, College Park, using the APs that are already deployed there and measuring the signal strength using a laptop with a network access card. The results of this study are presented in this thesis.

1.3 Thesis Outline

In Chapter 2, I present some past work and related reading. In Chapter 3, I discuss the basic physical concepts behind this problem. In Chapter 4, I delineate my theoretical model and some results. Some empirical studies conducted for verification of the model are presented in Chapter 5. Some theoretical implications of this model are presented in

Chapter 6. In Chapter 7, I examine the effect of the presence of obstructions in the path of the RF radiation. I conclude in Chapter 8 and discuss future directions.

Chapter 2. Related Work

The area of modeling radio wave propagation has been studied by many researchers and from a variety of perspectives. When such studies were conducted for supporting the design of a system, the aim usually was to come up with empirical models which could be used in practice to engineer the systems. Many of these studies have been conducted to support the design and implementation of cellular telephone systems [e.g. 17]. Recently some studies have been conducted looking at the signal propagation in an indoor environment also.

In [1], a review of popular propagation models for the wireless communication channel is undertaken. Macrocell (typically a large outdoor area), microcell (a small outdoor area), and indoor environments are considered. In the first case, LoS conditions are usually not satisfied. The signal propagates by reflection, diffraction and refraction. Since there are so many factors, creating a model is difficult, but a few have been proposed. The microcell model is easier to formulate, both from empirical results, and by physical analysis. For example, an empirical model is proposed in [2]. A 'ray-optic' theoretical model is proposed in [3].

Several studies have indicated that indoor propagation models can be difficult to formulate and use. Field strength measurements [4] show that fluctuations can be very high (up to 80dB). Parameters used in empirical models require more compensation to fit experimental data than for the outdoor situations. This phenomenon is attributed to the

fact that at a particular point, the signal strength is determined by a much larger number of indirect components.

There are two types of models to fit behavior – experimental/statistical[1] models, and theoretical models[2]. Many experimental models are based on measurements. A model is formulated to fit the data. For example [5] proposes:

$$PL(d) = PL(d_0) + 10*n*\log(d/d_0) + A \qquad (2.1)$$

Where $PL(d)$ is path loss in dB at distance d, $PL(d_0)$ is the known path loss at reference distance d_0, n is the exponent depending on propagation environment, A is uncertainty in model. Parameter n is very sensitive to propagation environment – type of construction material, type of interior, relative location within building etc. n ranges between 1.2 (waveguide effect[3]) to 6. These models have a significant error rate.

A few studies have used analytic models. In the ray-tracing model (e.g. [6]), all possible signal paths from the transmitter to the receiver are calculated. Predictions can be based on free-space transmissions, reflections, diffraction, diffuse wall scattering, and transmission through various materials. At any point, the sum of all the components is taken to get the signal strength. This method can also be used to predict time dispersion

[1] In these the experiment is conducted, and mathematical formulae are inferred from the results.

[2] The model is created using principals of physics.

[3] Waveguides are typically tubular structures. Their characteristics are such that waves traveling in them are forced to follow their structure. This is an efficient mechanism for signal transmission, it reduces loss.

(signal fluctuation across time at a particular location). This model needs a very detailed analysis and can be computationally very expensive. Note that the approach I have taken in this thesis is similar to the one in this paper except that I do not use explicit ray tracing techniques.

In the finite-difference time-domain (FDTD) models, a numerical solution of Maxwell's equations is undertaken [7]. Maxwell's equations are approximated by a set of finite-difference equations. A numerical solution is obtained by finite differencing. This is also a computationally demanding method. It is only suitable for small areas. For larger sizes, ray-tracing models are considered better.

The theoretical models are computationally very expensive, and the empirical models are not very accurate. These limitations can be overcome by an artificial neural network model. The ETF- Artificial Neural Network(ANN) model [4, 8] is based onmultilayer perceptron feedforward neural networks. For a particular environment, the neural network has to be trained with measured data. While the training is expensive, it only needs to be done once. Experiments show that the accuracy of this model is comparable to the accuracy of the ray-tracing and FDTD models.

Other phenomena affecting signal transmission have been studied. E.g. in [4], it is seen that a receiver moving slowly within the indoor environment experiences Ricean or Rayleigh fading[4]. Faster moving receivers experience Doppler shifts. The presence of human beings in the experimental area affects the results also [9]. The user's own body

[4] These are mathematical equations modeling the fading.

(very close to the receiver) causes a drop in signal strength. Other people in the vicinity not only cause attenuation, but fluctuation also. These irregularities are hard to predict.

An interesting application of measurement and modeling of signal features is the field of indoor geolocation. (e.g. [10], [11]). Geolocation is the tracking of mobile human beings and objects within a building. An algorithm is introduced, (e.g. [11],[12]), signal measurements are made, and the locations are calculated. The measurements made may include [10] arrival distance of the signal, angle of arrival, signal strength, phase, time of arrival and so on. This is a complex scenario, so a variety of location finding algorithms have emerged e.g. [13].

We note that all these studies have looked at the RF propagation in different environments and have studied ways of predicting the signal characteristics taking into account the specific environment under study. In my study I consider a simple model of propagation in a 3D environment.

Chapter 3. Background

3.1 Wave Propagation and the Free Space Model

The starting point in this study is the wave propagation in free space. The signal at distance x from the source, $J(x)$, can be written as [18]-

$$J(x) = (J_0 x^{-D}) e^{i(2\pi f x c)} \qquad (3.1.1)$$

where

x = distance from source

J_0 = signal amplitude at source

f = frequency(2.4 GHz)

D = Exponent value contributing to decay of signal as a function of distance x

c = speed of light in free space

We note that for free space generally the value of D should be two. However, in several empirical studies researchers have proposed a number of other values for D, varying from 1.2 to 4, which reflect the specific environment that they were considering. I will start with the value of *D* as 2. Further, the signal $J(x)$ is treated as a complex variable and this aspect has to be taken into account when I manipulate this variable.

The basic premise of this study involves a transmitter/antenna/AP(access point) called **T** (this transmits the radio signal), and the receiver **R,** which is the recipient of this signal.

3.2 Indoor Environment

When a radio wave encounters objects in its path it gets affected by them. The most significant factors affecting the propagation of radio waves are *reflection, absorption, diffraction, scattering,* and *refraction* [15]. Let us consider these next.

3.2.1 Reflection

Reflection occurs when the radio wave is incident on a surface which has much larger dimensions than its wavelength. In an outdoor environment, these would occur off the surface of the earth, buildings etc. In an indoor environment, it would be walls, people and other obstructions. The reflected waves follow the typical laws of reflection in that the incident angle is equal to the angle of reflection and that the wave undergoes a phase change of 180 degrees. Depending on the material of the reflecting surface a portion of the signal may also be absorbed. Perfectly conducting materials are perfect reflectors, while poorer conductors involve more absorption of the signal before reflection. The conductivity of a material further depends on its dielectric properties.

3.2.2 Absorption

As the radio wave passes through a material, a portion of its energy is absorbed. The amount of absorption depends on the characteristics of the material.

3.2.3 Diffraction

This occurs when the radio path between the transmitter and the receiver is obstructed by a surface that has sharp irregularities (edges). The radio signal impinging on the edge results in secondary waves which propagate in all directions around the edge(including behind the obstacle.) This phenomenon is responsible for providing a path between the **T** and the **R** even when there is no direct or reflected path. The diffraction depends on the geometry of the object, as well as on the amplitude, phase, and polarization of the incident wave at the point of diffraction.[15]

3.2.4 Scattering

When there are objects of comparable dimensions to the wavelength of the radiation in the medium of transmission, scattering of the signal occurs off of these objects. If the number of such objects per unit volume is large, the effects of scattering can be appreciable. Scattering is particularly prevalent when there are rough and irregular surfaces present.

3.2.5 Refraction

In an outdoor environment, the atmosphere has a refractive index, which curves the path of the signal. This changes the geometry of the situation. In an indoor environment, this effect is not significant. However, the signal does pass through objects, within which

refraction will occur. So the signal will come out at a different position than expected. Thus, obstructions change the path of the radiation.

3.3 The Multipath Effect

As a consequence of the factors noted in section 3.2, the receiver **R** may get multiple waves following different paths, from the source **T** to it. Each of these waves will have its own amplitude and phase, and will arrive at **R** with its own delay. Note that the signal received at **R** is the superposition of all these component waves obtained by adding the signal values treated as complex numbers. I can then determine the signal strength as the amplitude of the complex number.

Chapter 4. Theoretical Model

4.1 Basic Premise

Given a rectangular 3-D space whose dimensions are known, and with a radio wave transmitter and receiver of known coordinates, I calculate the field strength at every point in this space by taking into account the direct **LoS** ray and the reflected waves reaching the receiver. I only consider the waves reaching the receiver after one reflection.

4.2 The Environment

In this study I consider a rectangular 3-D space to model a corridor in a building (this space is now called the 'box') in which one AP has been installed at a fixed location. The dimensions of the corridor and the location of the AP are known. I proceed to calculate the signal strength measured at a location in the box by taking into account the direct LoS path and 6 reflected waves.

I assume that the corridor walls are parallel to the axes of the coordinate system and that the origin is at one corner, x-axis is along the length, y-axis is along the width and z-axis vertical in this box. Further,

- The corridor has dimensions *A, B, C*.
- The access point coordinates are *x1, y1, z1*.
- The receiver coordinates are *x2, y2, z2*.
- The walls have reflection coefficients of rc_1.

- The floor has a reflection coefficient of rc_2.
- The ceiling has a reflection coefficient of rc_3.
- The original amplitude, as emitted by **T**, is given by J_0.

4.3 Paths Traveled by the Waves

Let us look at the different paths taken by the rays to travel from transmitter to receiver as in Fig 4.1 and Fig. 4.2

- **LoS** (line of sight) path between ***T*** and ***R*** called ***T-R***. Let this distance be *d1*.

Clearly this distance can be calculated as

$$d1 = \sqrt{(x2 - x1)^2 + (y2 - y1)^2 + (z2 - z1)^2} \qquad (4.3.1)$$

- ***R*** also receives 6 different rays from reflections. These are paths traveled by rays from ***T*** to each separate plane in the box and then reflected back to ***R***.

In order to consider the reflections let us examine one pair of reflections. They are off of 2 planes – the $y = 0$ plane, and the $y = B$ plane. Consider a ray that starts from **T**, then impinges on surface $y = 0$, undergoes reflection, and then reaches **R** , the receiver. The diagram(Fig. 4.1) shows this.

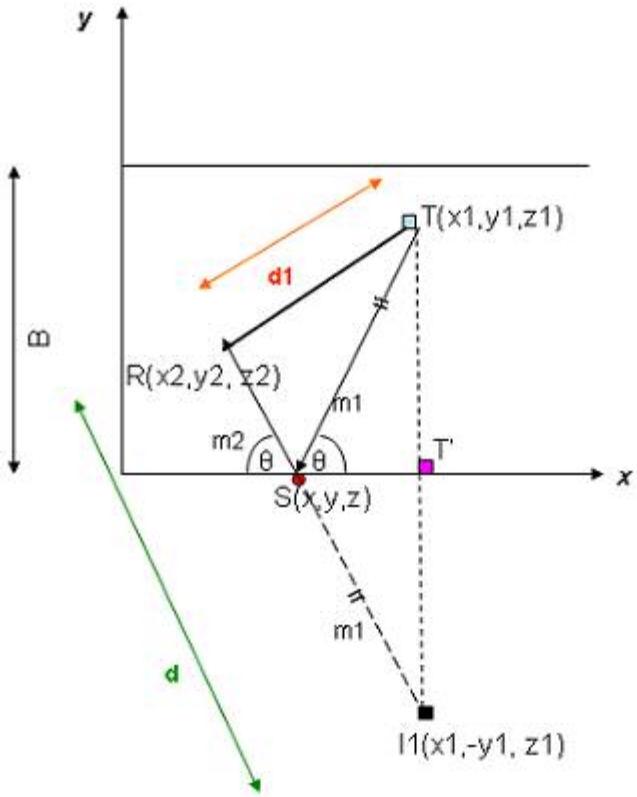

Fig. 4.1 Reflection from y = 0 plane

The point of reflection is S(*x, y, z*). As we note from the equation for the signal strength, the main factor to consider for the reflected wave is the total distance traveled and the loss at the point of reflection. A phase change of π also has to be added. In order to calculate the distance traveled I draw the 'image' of the transmitter on the other side of the x-axis.

For the reflection, the distance traveled by the ray is ***T-S + S-R***. Looking at the diagram, from simple geometry, it can be seen that this is equal to ***I1-R***. So *d*, distance traveled by the ray reflecting off of *y = 0* plane, is *x2*

$$d = \sqrt{(x2 - x1)^2 + (y2 + y1)^2 + (z2 - z1)^2} \qquad (4.3.2)$$

Now for the $y = B$ plane. Refer to diagram Fig. 4.2.

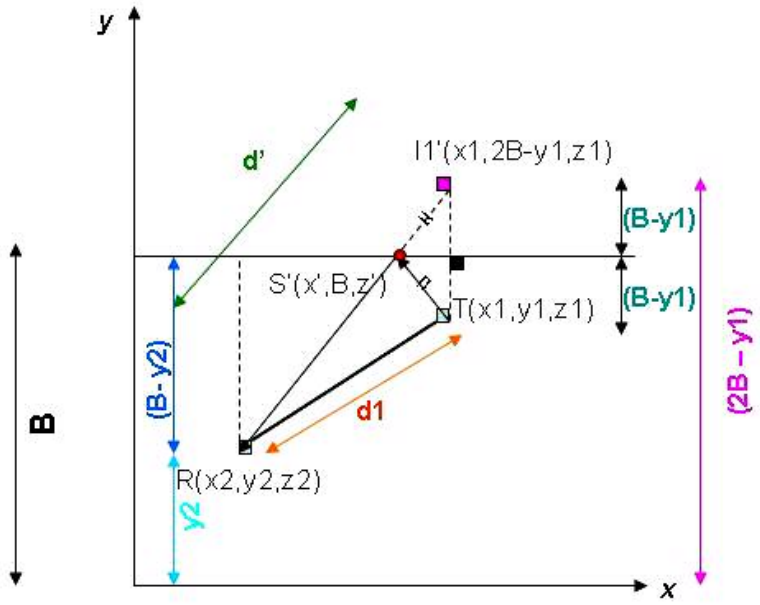

Fig. 4.2 Reflection from y = B plane

The point of reflection is *S'(x',B,z').* So, *d*', the distance traveled by the ray reflecting off of $y = B$ plane, is I1'-R, which is

$$d' = \sqrt{(x2 - x1)^2 + (y2 - 2B + y1)^2 + (z2 - z1)^2} \qquad (4.3.3)$$

The other reflected distances (from the other planes) can be calculated analogously.

4.4 Magnitude Calculation

As noted in Chapter 3, the signal strength at any point, with attenuation due to distance, is given by

$$J(x) = J_0 x^{-D} e^{(\frac{2\pi fx}{c})} \qquad (4.4.1)$$

Where

x = distance from source

J_0 = signal amplitude at source

f = frequency(2.4 GHz)

D = exponent value contributing to decay of signal

As a function of distance x

c = speed of light in free space

By Euler's equation, this can be rewritten as

$$J(x) = J_0 x^{-D}[Cos(\frac{2\pi fx}{c}) + iSin(\frac{2\pi fx}{c})] \qquad (4.4.2)$$

- For the **LoS** path, using eqn (4.3.1), the amplitude at **R** due to this ray is given by

$$J(R) = J(T)d1^{-D} e^{(\frac{2\pi fd1}{c})}$$

Or

$$J(R) = J(T)d1^{-D}[Cos(\frac{2\pi fd1}{c}) + iSin(\frac{2\pi fd1}{c})] \qquad (4.4.3)$$

- Consider the case of the reflections.

The 2 rays travel distances of d and d' respectively (as in *(4.3.2)* and *(4.3.3)*).

The amplitude at **R** due to the reflected ray having traveled distance *d* is–

$$J(R) = J(T)rc.d^{-D}e^{(\frac{2\pi fd}{c}+\pi)} \qquad (4.4.4)$$

This can also be written as(for a reflection off a wall which has reflection coefficient rc_1)

$$J(R) = J(T)rc_1 d^{-D}[Cos(\frac{2\pi fd}{c}+\pi) + iSin(\frac{2\pi fd}{c}+\pi)] \qquad (4.4.5)$$

So we have seven rays arriving at ***R***. We calculate the real and imaginary parts of each ray using the sine and cosine components .So we have r1….r7 real contributions, and im1….im7 imaginary contributions.

$$Real = r1 + r2 + r3 + r4 + r5 + r6 + r7$$

$$Img = im1 + im2 + im3 + im4 + im5 + im6 + im7 \qquad (4.4.8)$$

The total magnitude is calculated as

$$Magnitude = \sqrt{Real^2 + Img^2} \qquad (4.4.9)$$

In this way we can calculate the magnitude of the signal received at any arbitrary point.

Chapter 5. Experiments

In order to verify the applicability of the model developed in Chapters 3 and 4, I conducted some experiments by measuring signal strengths in a corridor in the AV Williams building. I used the AP installed in that corridor for the UMDnet and measured the signal strength by placing a laptop with a network interface card at measured locations. I used a software package called Horus[5] to take the measurements. At each location, 300 readings of the signal strength were taken in 100 seconds. From these readings, I obtained the average signal strength as well as the standard deviation at each location.

Note that while the model used is deterministic, in practice there are noise factors that affect the signal strength. These include the movement of objects around the receiver during the measurement, and also receiver and antenna noise. These noise factors will give rise to variability in the results. I expect the model to capture the average behavior of the measurements. However, I will indicate the standard deviation of the measurements in my results.

When making the model calculations I used the following parameter values which are based on some published results:

- The decay exponent $D = 2$. This is as indicated for Eqn. 3.1.1.(Though I will modify this and indicate if I have done so)

[5]Developed by Dr. Moustafa A. Youssef, University of Maryland at College Park

- The walls have reflection coefficients of $rc_1 = 0.5$.
- The floor has a reflection coefficients of $rc_2 = 0.3$.
- The ceiling has a reflection coefficient of $rc_3 = 0.1$.

(The reflection coefficients are as used as in [16].)

In a later section, I will look at the impact of model parameter values and how better values can be selected for my experiments.

There are some other factors that the model does not directly account for. These include antenna and receiver gain, system losses, absorption, and noise factors. I expect this to contribute to a linear shift, or difference between the model and experimental results. I will experimentally determine the magnitude of this shift, and will shift the value of the model plot accordingly.

5.1 Experiment 1

The experiments were conducted in a corridor on the 4th floor of the AVW Building.

5.1.1 Experimental Setup

The corridor layout is shown in Fig. 5.1.

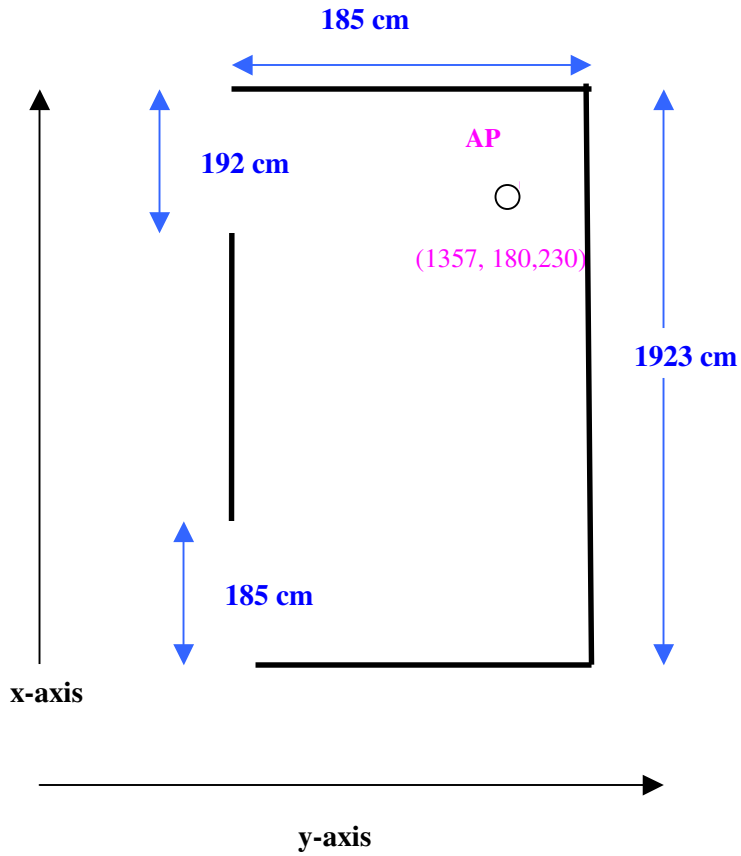

Fig

. 5.1 Room Layout

The corridor I used for the measurements had length 1923 cm and width 185 cm. The height of the room was 248 cm. The x- and y- axes were chosen as indicated in Fig. 5.1. The z-axis was chosen to be perpendicular to the floor. The 192 cm and 185 cm correspond to gaps in the walls for the corridors leading out of this space. (I chose measurement locations such that no reflected rays affecting the data points would be incident on those areas). The AP is marked in the diagram and had coordinates of (1357, 180, 230). The experimental setup was as in Fig. 5.2.

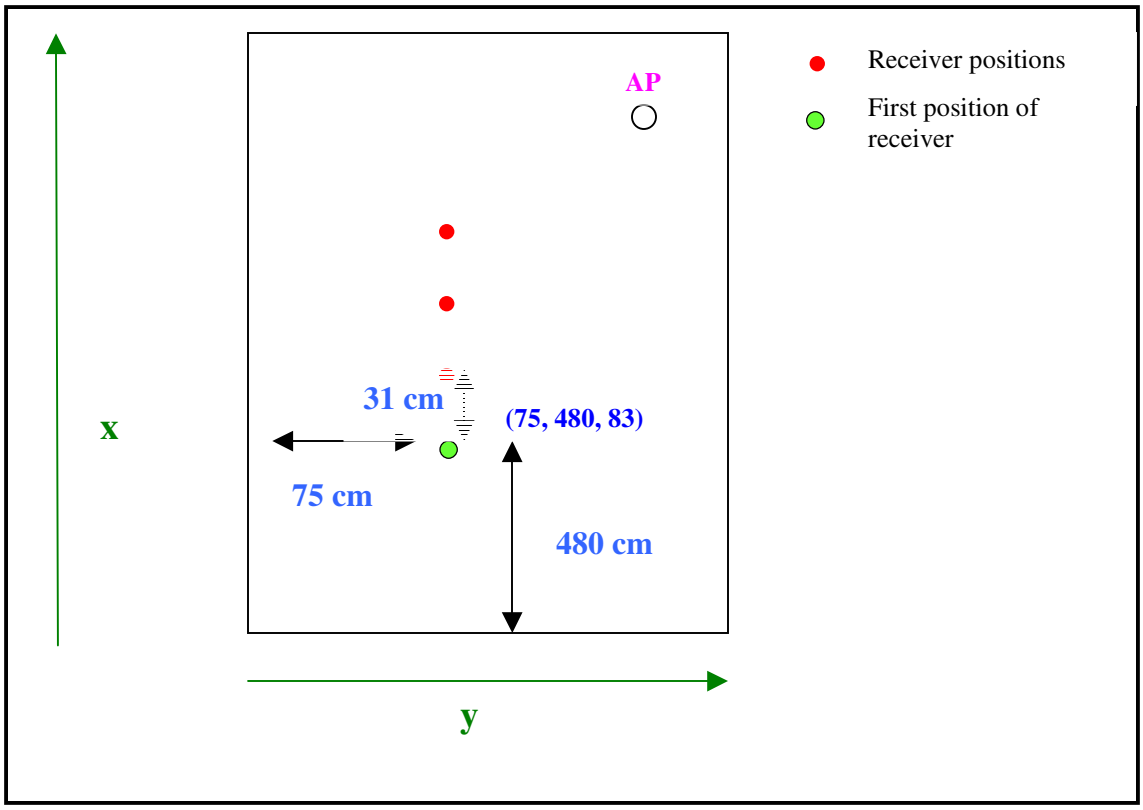

Fig. 5.2 Experimental setup

In Fig. 5.2, the x- and y- axes are as marked. The first position of the receiver was the green dot, and its position coordinates are shown. The subsequent positions were the red dots. All measurements were taken by placing the laptop on a trolley so that the NIC was at a height of 83 cm.

At the first point, the receiver coordinates were (480, 75, 83). I moved the cart to increment the x-position (by 31 cm each time), and measured the magnitude at each point.

5.1.2 Results

The value of the signal strength at each point was measured. The experiment was repeated . So there are two sets of measurements. The results for the first set of experiments are plotted in Fig. 5.3.

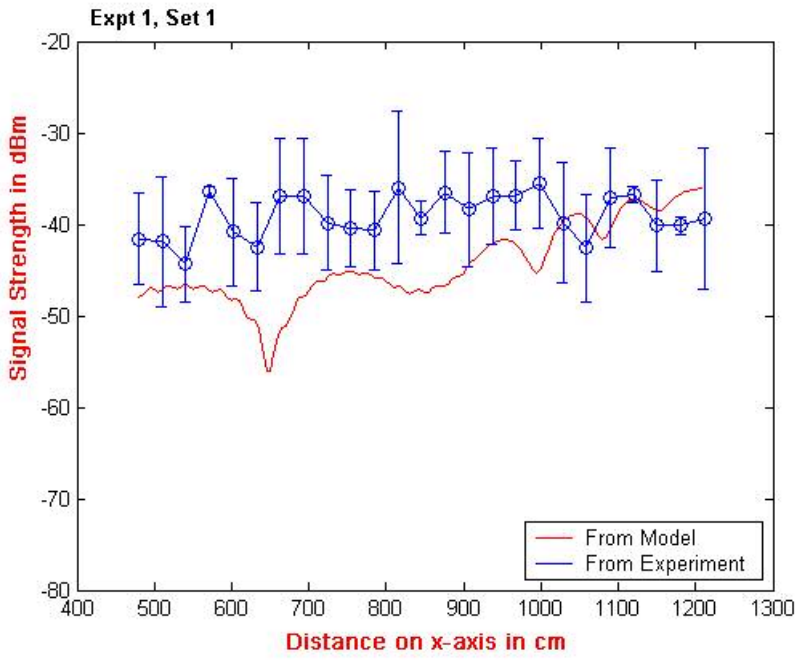

Fig. 5.3 Signal values from Model and from Experiment

The errorbars show measured signal strength values within one sigma bound of the mean value. The rms error between experiment and model is 6.23 dBm.

I include the results from the second set of measurements(Fig. 5.4). This set of measurements was taken immediately after the first one. I take multiple sets to observe the variability of results for the same experiment repeated with the same setup.

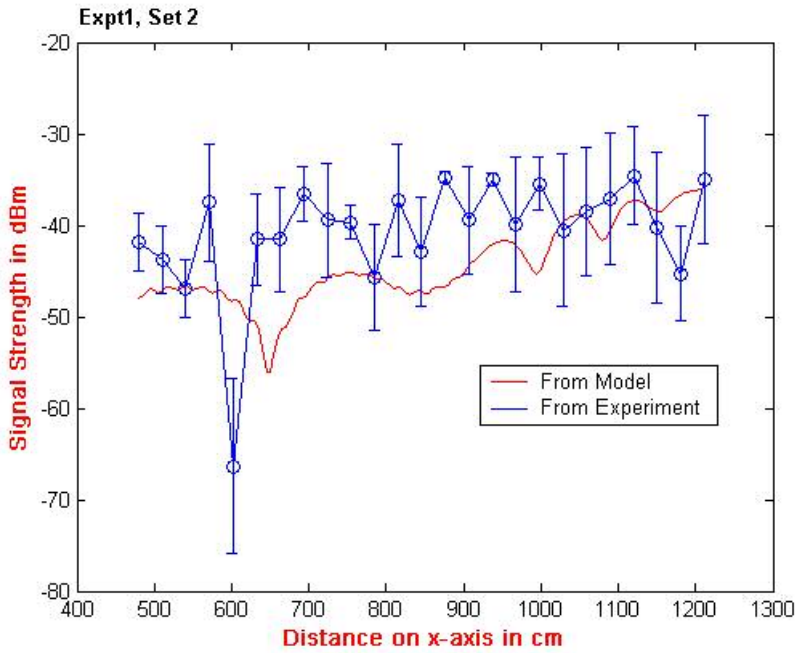

Fig. 5.4 Signal values from Model and from Experiment

The rms error between experiment and model is 6.08 dBm. The 5th data point has an unexpected dip in value.

It is noted that there is attenuation in the signal with increasing separation from the antenna, as expected. Also, data points exhibit dips and peaks in the signal strength, and this can be attributed to variations introduced by the multipath effect.

5.1.3 Model Parameter Adjustment

I shall examine if a better fit to experimental data can be obtained by adjusting the values of parameters used in the model.

- Decay exponent, D

From first principles, the decay exponent should have value 2. However, it has been hypothesized in the literature [15] that a decay exponent other than 2 should be used. I shall vary the value of D until a good fit with experiment is observed.

- Reflection coefficients rc_1, rc_2, rc_3 .

In the model plots that I have drawn so far, I used reflection coefficients of 0.5, 0.3, and 0.1 as indicated in [16]. However, in our setup, these may consist of different values. So I should vary the values of these coefficients until a good fit with experiment is obtained.

I proceed to vary all the parameters together until a best fit is obtained. I vary D from 0.2 to 2.0, and each of the rc values from 0.1 to 0.9.

For the first set, I get a best fit at $D = 0.6$, $rc_1 = 0.1$, $rc_2 = 0.1$ and $rc_3 = 0.1$. I shift the graph by 32.87 dBm. The rms error is 2.26 dBm.(Fig.5.5)

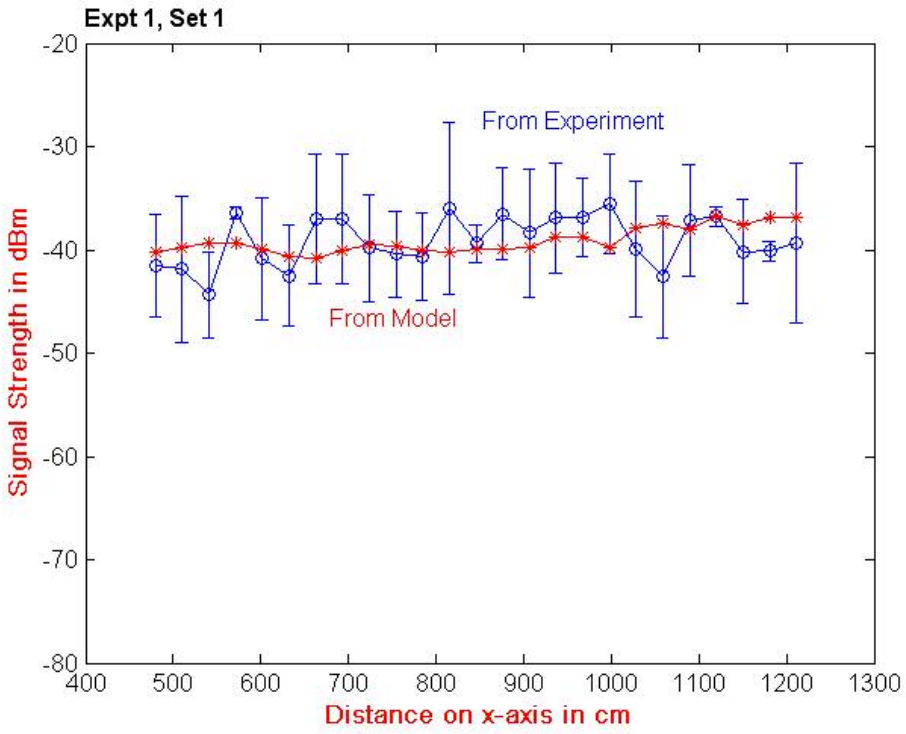

Fig 5.5 Signal values from Model and from Experiment

It is seen that values predicted by the model now lie entirely within the range of experimentally measured values.

For the second set, I again vary the D and rc's as previously. The best fit is obtained with at $D = 0.8$, $rc_1 = 0.1$, $rc_2 = 0.1$ and $rc_3 = 0.1$. The graph hasis shifted by 29 dBm. The rms error is 3.82 dBm.(Fig.5.6)

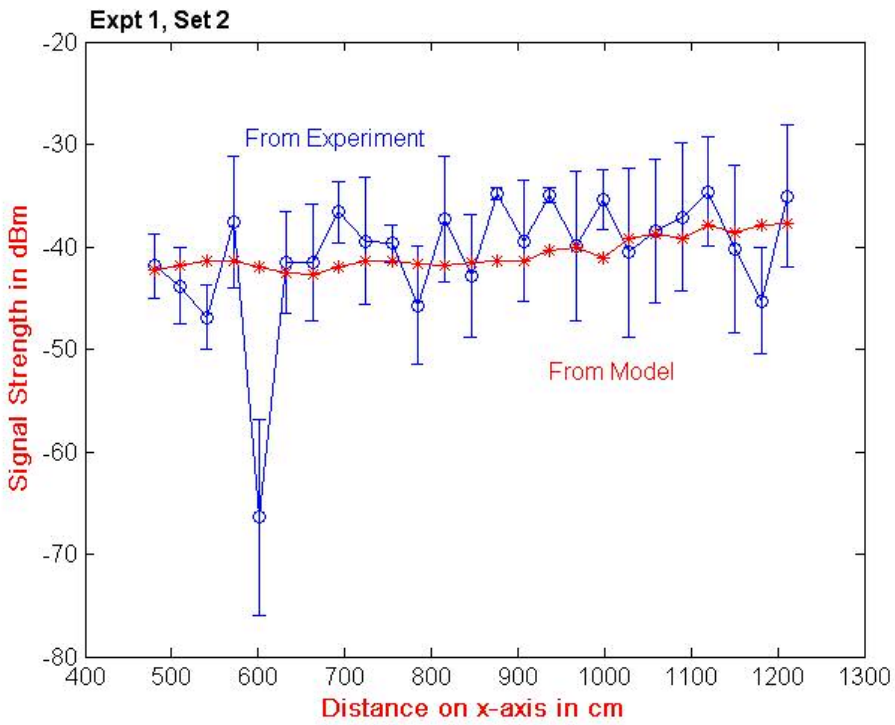

Fig. 5.6 Signal values from Model and from Experiment

Again, it is seen that values predicted by the model lie almost entirely within the range of experimentally measured values.

5.1. Both Sets of Data

I plot both datasets together to get Fig.5.7. I will use the average of the parameter values used so far(D = 0.7, rc_1 = 0.1, rc_2 = 0.1 and rc_3 = 0.1, shift = 31 dBm).

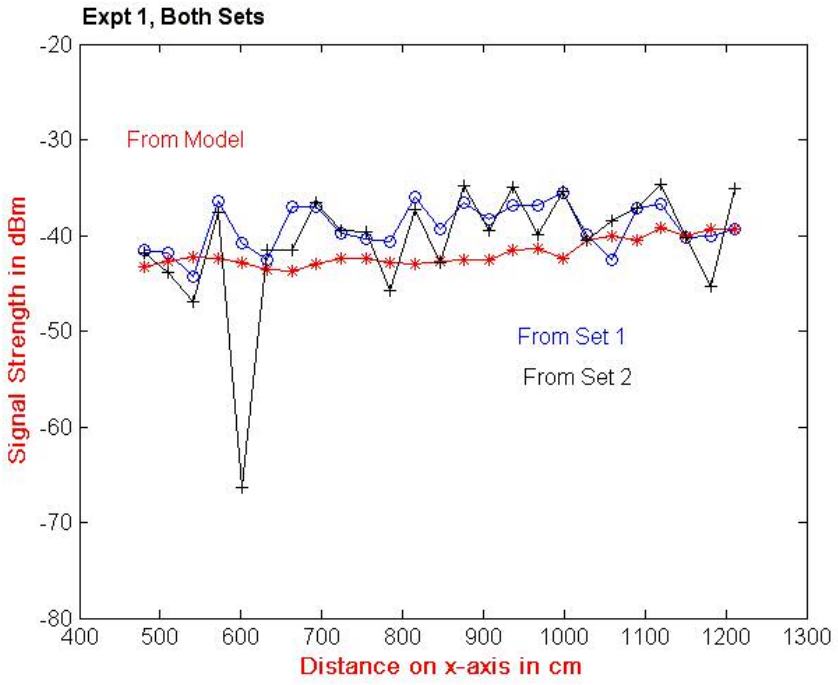

Fig. 5.7 Signal values from 2 Datasets and from Model

It is seen that (except for a few deviant points) data from the different datasets are relatively close together. Clearly there are other factors at work which impact the actual measured values. Let us look at some of them next.

5.1.5 Sources of Error

There are errors in my measurement process which have not been accounted for.

- Errors manifest as a result of receiver and antenna noise. Also there is error due to people walking around and obstructing the rays. These will manifest as the variance in the measurements made.

- Positional errors

These are the errors in the measurement of room dimensions, and antenna and receiver coordinates. I shall consider only the last item, as the receiver position is constantly changed, and there is more chance of error.

I recalculate values generated by the re-parameterized model (with the optimal D , rc's, and shift, as obtained from the last two sets of the experiment), and with the introduction of a jitter value in the receiver coordinates (Fig. 5.8). I allow a jitter value of +- 7cm in each coordinate direction (y- and z- coordinates).

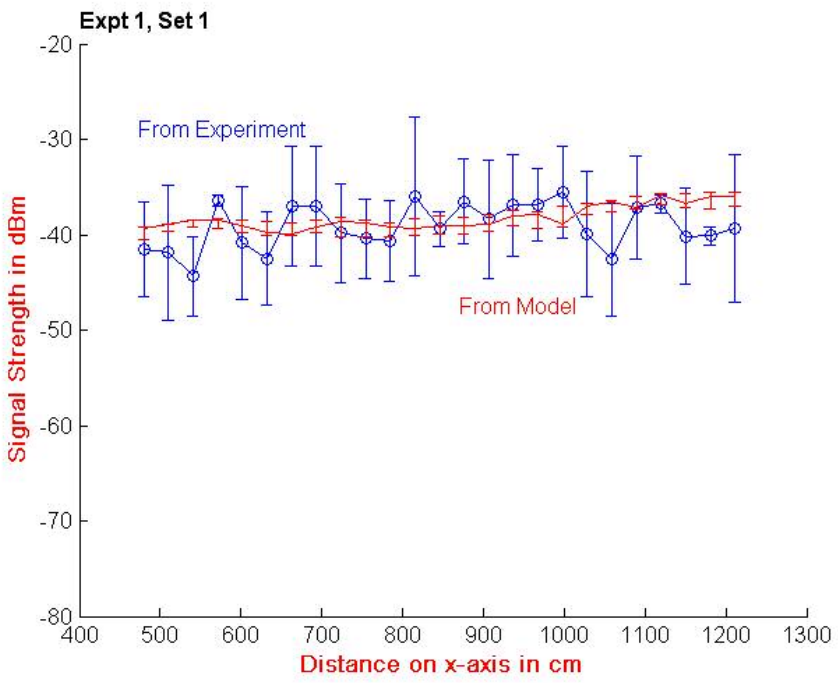

Fig. 5.8 Values with jitter in receiver y- and z- coordinate values

[AKA1]

The values in the errorbars in the plot of the model indicate the range of values obtained by jittering the receiver coordinate values. It is seen that variability is introduced due to

position jitter. The range of model values still liealmost entirely within the range of experimentally observed values when the **R** position error is included in the graph.

I repeat this for the second set of measurements as shown in Fig. 5.9.

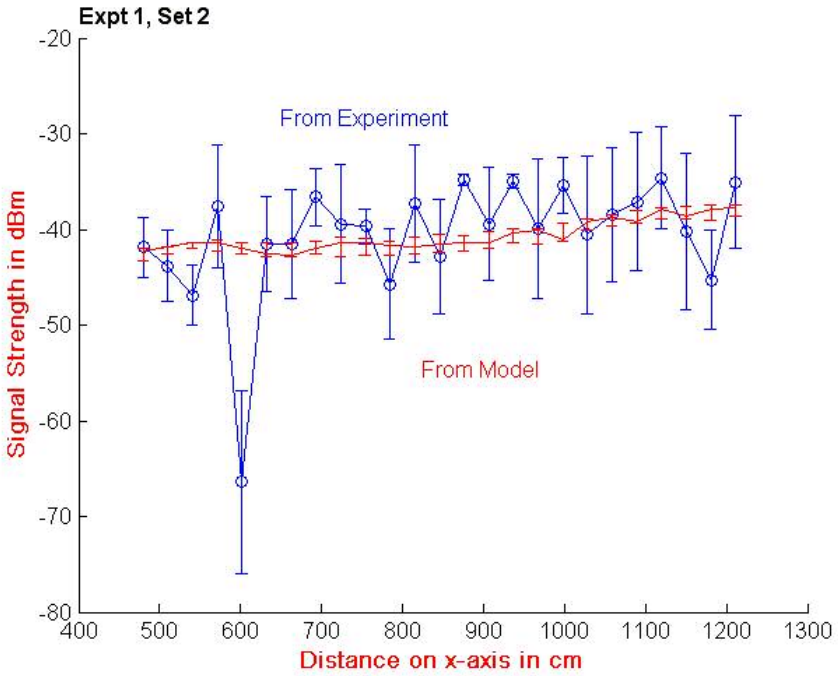

Fig. 5.9 Values with jitter in receiver y- and z-coordinate values

Some variability is introduced due byposition jitter. Again, the model values still lie almost entirely within the range of experimental values.

It is seen that location error introduces some variability into the model results.

5.2 Experiment 2

The experiment was repeated in the same corridor with different receiver locations.

5.2.1 Experimental Setup

The receiver position was again varied only on the x-axis. As before, antenna coordinates were (1357, 180, 230). The first position of the receiver was at (345, 83, 91). The receiver was moved by 31 cm each time, and I had 40 data points. Two sets of measurement were made.

5.2.2 Results

I plot the results. I directly optimize the values of D, rc's, and shift (Fig. 5.10).The results from the first set of experiments are plotted in Fig. 5.10 For the first set, the best fit is obtained with at $D = 0.8$, $rc_1 = 0.3$, $rc_2 = 0.3$ and $rc_3 = 0.1$. The graph is shifted by 26.2 dBm. The rms error is 2.63 dBm.

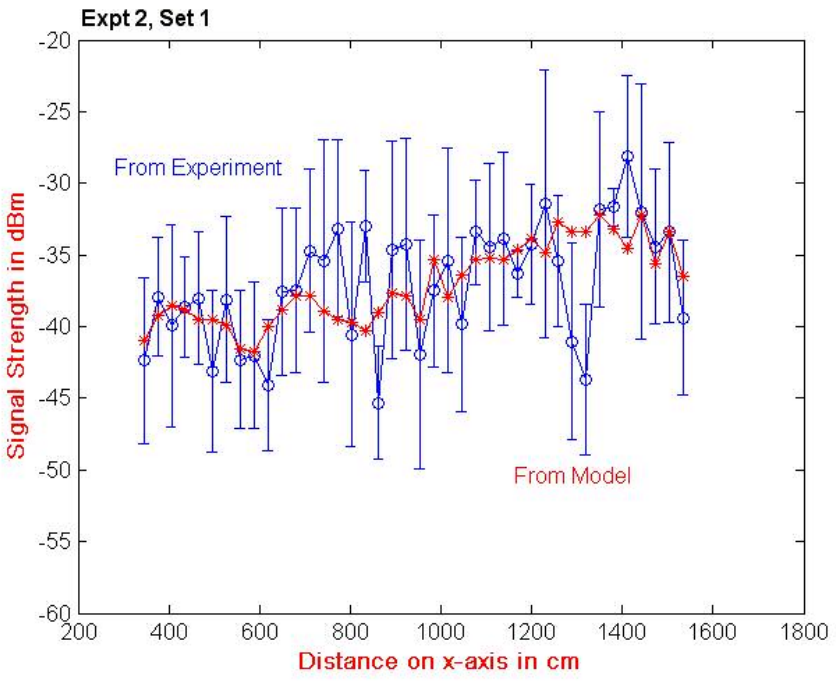

Fig. 5.10 Signal values from Model and from Experiment

There is excellent agreement between experiment and the adjusted model.

I took another set of measurements, as plotted in Fig. 5.11. the best fit is obtained with at $D = 0.8$, $rc_1 = 0.3$, $rc_2 = 0.1$ and $rc_3 = 0.1$. The graph is shifted by 26.2 dBm. The rms error is 2.14 dBm.

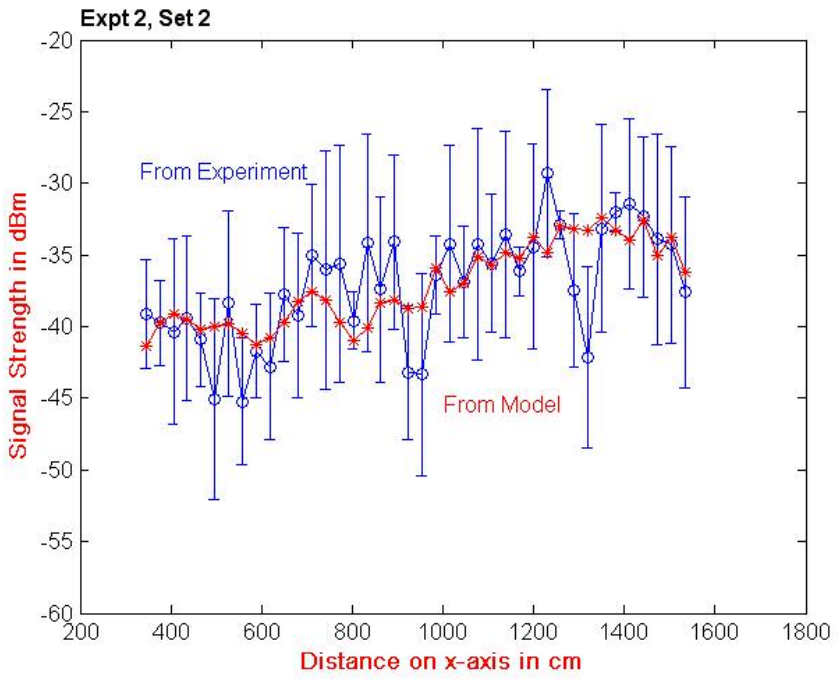

Fig. 5.11 Signal values from Model and from Experiment

Again, there is an excellent match between theory and experiment.

I plot both datasets together in Fig. 5.12. For the parameter values, I use the average of the last two sets and use D= 0.8, $rc_1 = 0.3$, $rc_2 = 0.2$ and $rc_3 = 0.1$, shift = 26.2 dBm. I get Fig. 5.12.

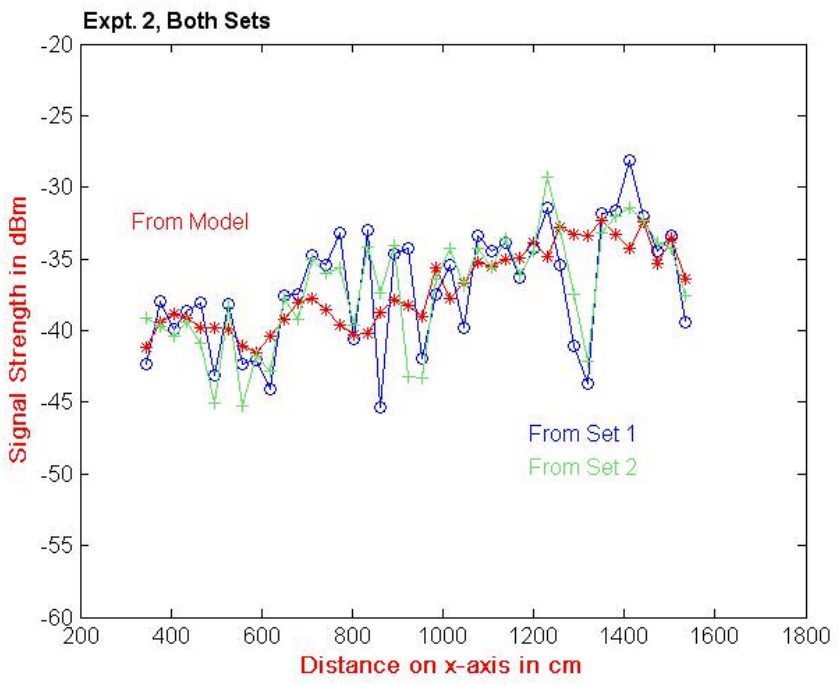

Fig. 5.12 Signal values from 2 Datasets and From Model

It is again seen that mostly, data from the different datasets are very close together.

5.2.3 Location Jitter

I consider errors in the measurement of **R** as before. I introduce a jitter(of +- 7cm) in the receiver coordinate positions, and regenerate the model graph .(I use the average values of D , rc's, and shift as obtained from the previous two sets of this experiment.)

For Set 1, I get Fig. 5.13

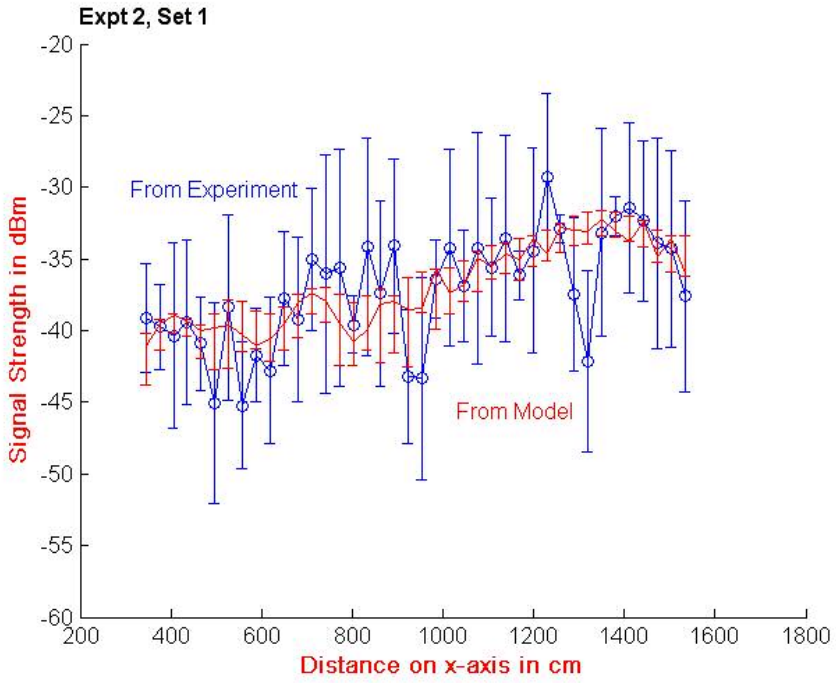

Fig. 5.13 Values with jitter in receiver y- and z- coordinate values

It is seen that the model values lie almost entirely within the range of experimental values.

I repeat this procedure for Set 2 to get Fig. 5.14.

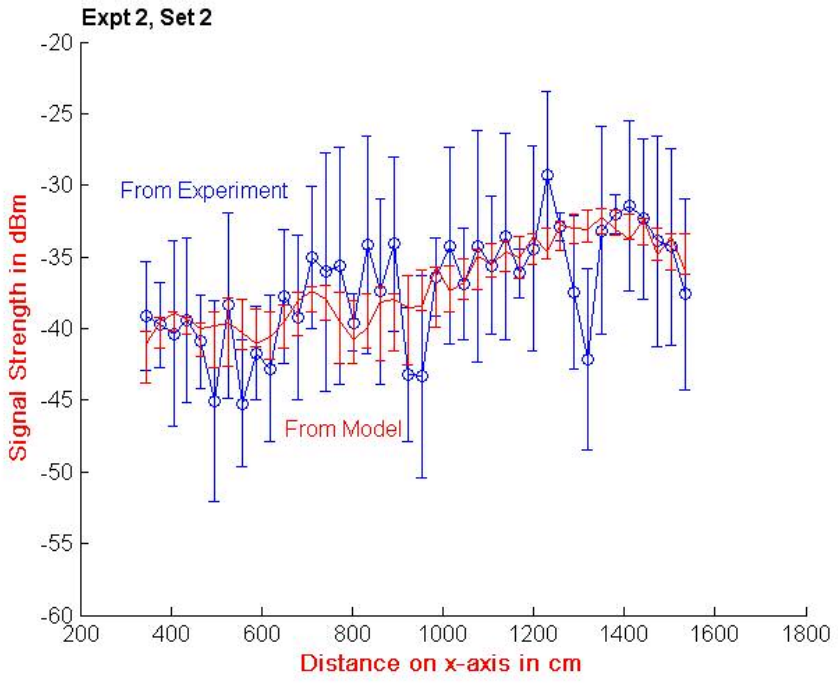

Fig. 5.14 Values with jitter in receiver y- and z- coordinate values

Again, it is seen that the model values lie almost entirely within the range of experimental values.

5.3 Re-Parameterized Model

So far, I adjusted some parameter values in my model to get a good fit to the data of Experiments 1 and 2. Over the two experiments, the average value of the decay exponent *D* is 0.75. The values of the reflection coefficients are 0.2, 0.15 and 0.1.The average value of the linear shift is 28.5 dBm. I shall use these values from now on.

5.4 Model Verification

I shall verify my re-parameterized model against another experiment.

5.4.1 Experimental Setup

This was conducted in the same corridor as in the previous two experiments. The initial position of the receiver was at (348, 105, 98) with increments of 31 cm along the x-axis happening each time. 22 measurements were taken.

5.4.2 Results

For the first set, I plot the experimental and model results in Fig.5.15. (The model uses the parameters as explained earlier.

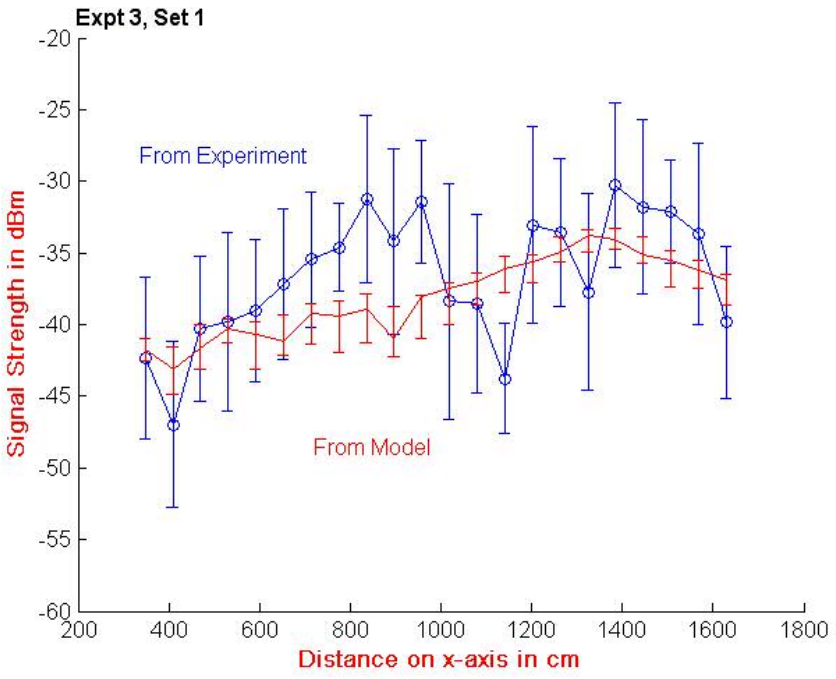

Fig. 5.15 Signal values from Model and from Experiment

The rms error is 3.6 dBm. The values predicted by this model lie somewhat within the range of values as measured by experiment.

Another set of measurements was taken as shown in Fig. 5.16.

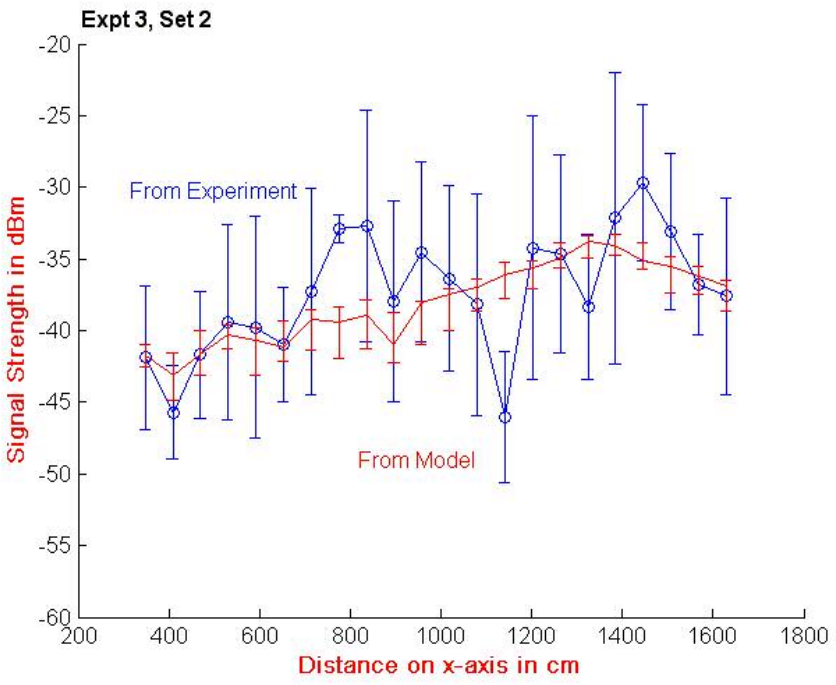

Fig. 5.16 Signal values from Model and Experiment

The rms error is 2.7 dBm. The values predicted by this model are largely within the range of values as measured by experiment.

5.5 Conclusions

It is seen that there is a good match of predictions of my model with experimental results. While the match is not perfect, it is well within experimental errors. Therefore I conclude that the model with adjusted parameters is useful in determining the signal strength in an indoor corridor.

Chapter 6. Model-Based Analysis

In this chapter I undertake further investigation into the effects of the analytic model. First, this gives us insights into the working of the model. Next, it helps us understand the salient features of the 3-D signal strength topology. Since the model results match the measurements well, we can use my model to predict signal strengths in an indoor environment. Further, it gives us ideas into future improvements of the model. Note that I use the re-parameterized model of Chapter 5. (The value of the decay exponent *D* is set at 0.75, the reflection coefficients at 0.2, 0.15 and 0.1, and the linear shift at 28.5 dBm.)

6.1 One Axis Variations

For Fig. 6.1, I use the data (receiver coordinates, antenna location, room coordinates) from Experiment 1 in Section 5. However, I extend the range of the readings for receiver x-values continuing beyond that of the x-position of the antenna. Also, a finer-grained set of x-positions are considered. I model the magnitude due to the LoS or direct line-of-sight ray, and also the composite magnitude containing all 7 rays in the model.

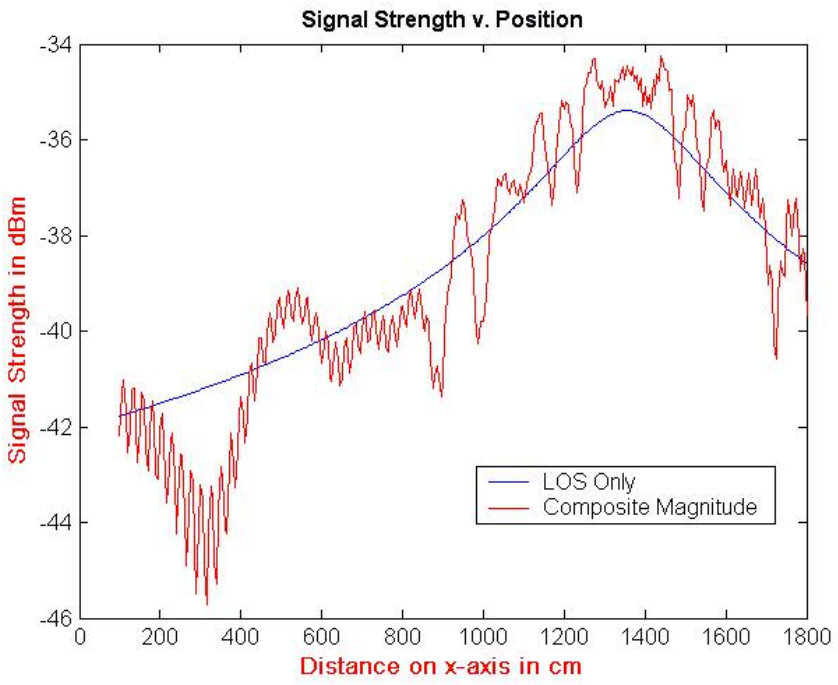

Fig. 6.1 Signal strength as predicted by model

Note that the AP is at x = 1357 cm. The model shows that the signal strength (both LoS and composite components) increase with proximity to the antenna, as expected. The LoS component is smooth, whereas the composite magnitude shows a lot of fluctuations due to the interference caused by the reflected waves. I evaluated signal strengths for this configuration for some other values of y and z, and found thata similar variability is observed.

To understand the signal characteristics, I also consider the signal strengths for variations along the other axes. I vary the y-coordinate smoothly keeping the x and z constant at x = 650 cm and z = 83 cm(Fig. 6.2)

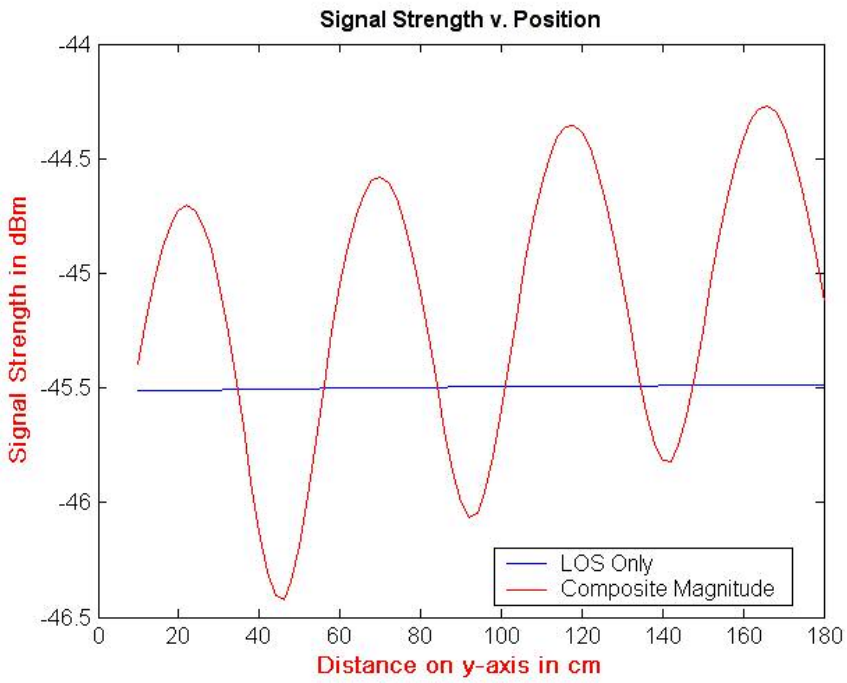

Fig. 6.2 Signal strength V. y-coordinate

There is a repetitive variation across the y-axis. There are drops of ~ 2 dBm over distances of ~ 20 cm.

Next, x and y are kept constant at x = 950 cm, and y = 160 cm. Varying the z-coordinate, I get the results shown in Fig. 6.3.

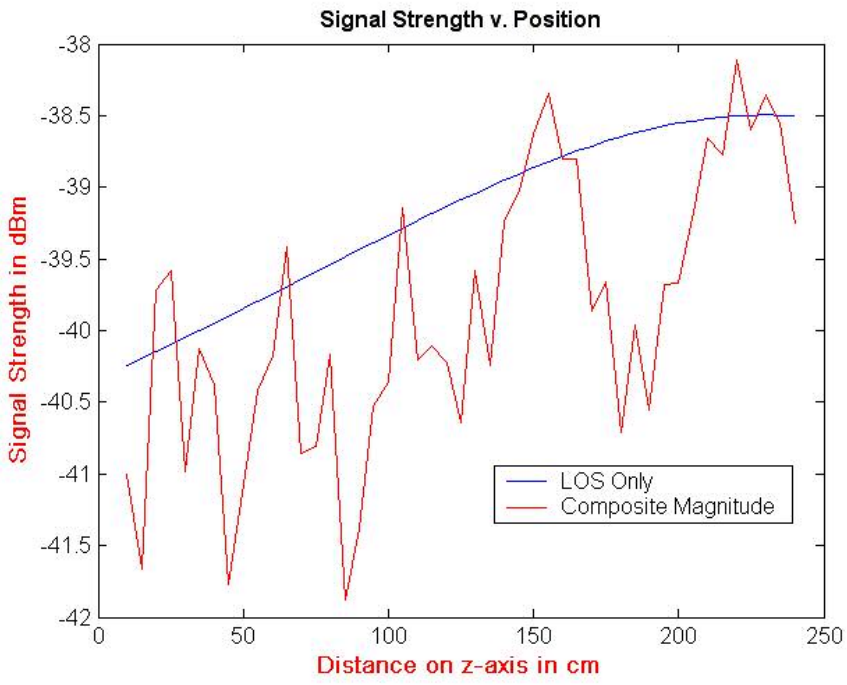

Fig. 6.3 Signal Strength v. z-coordinate

The magnitude of the LoS signal is mostly greater than that of the composite signal. This can be attributed to the geometry of the situation again.. The gross trend of the LoS signal gradually increases with increase in z-coordinate (increasing proximity to AP which is at z = 230 cm There are many jagged variations across the z-axis. There are changes of ~ 3 dBm over 20 cm.

Going back to Fig.6.1, I investigate the composite magnitude variations further. I zoom in on a portion of the graph to get Fig. 6.4.

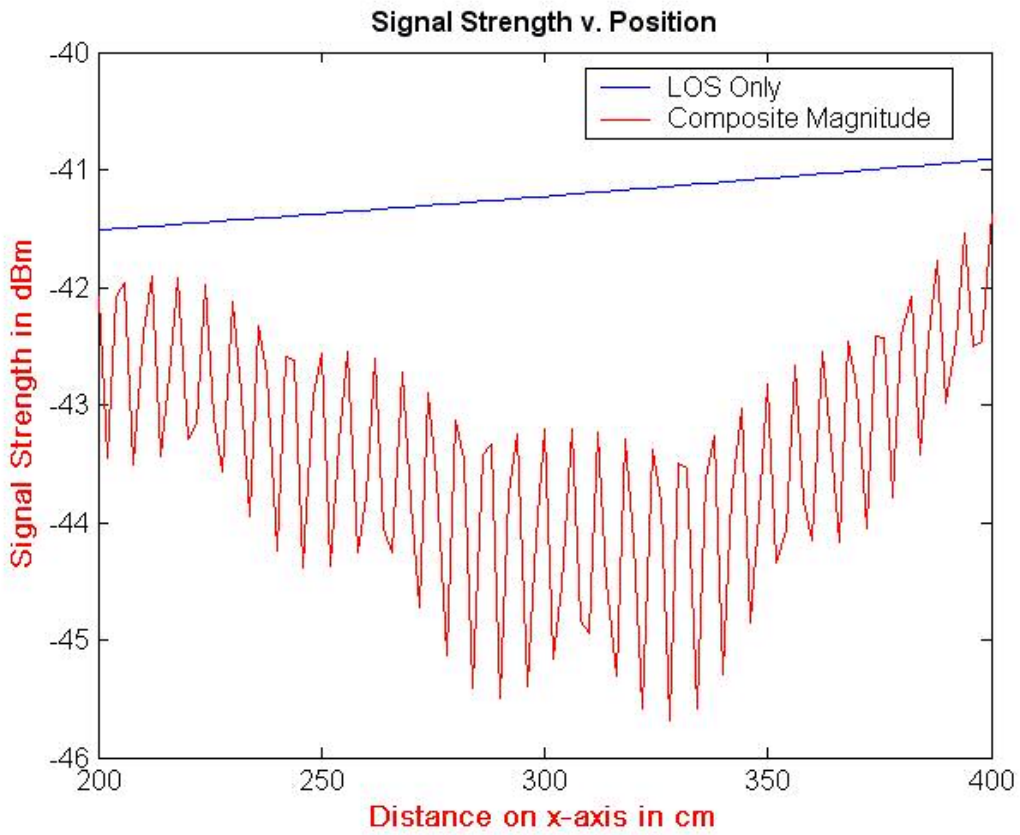

Fig. 6.4 Zoomed in signal strength

There are sharp, repetitive variations over short distances. The signal strength is sensitive to position on x-axis and a change in position of ~2 cm can cause a fluctuation of ~ 4 dBm.

Next let us look at the reflected waves separately. It is interesting to see the constituent signal strengths, and to see how they add up.

I split up the magnitudes due to each pair of reflected rays (off of 2 facing walls). The results from the 3 sets of reflections are shown in Fig. 6.5 (a),(b) and (c).

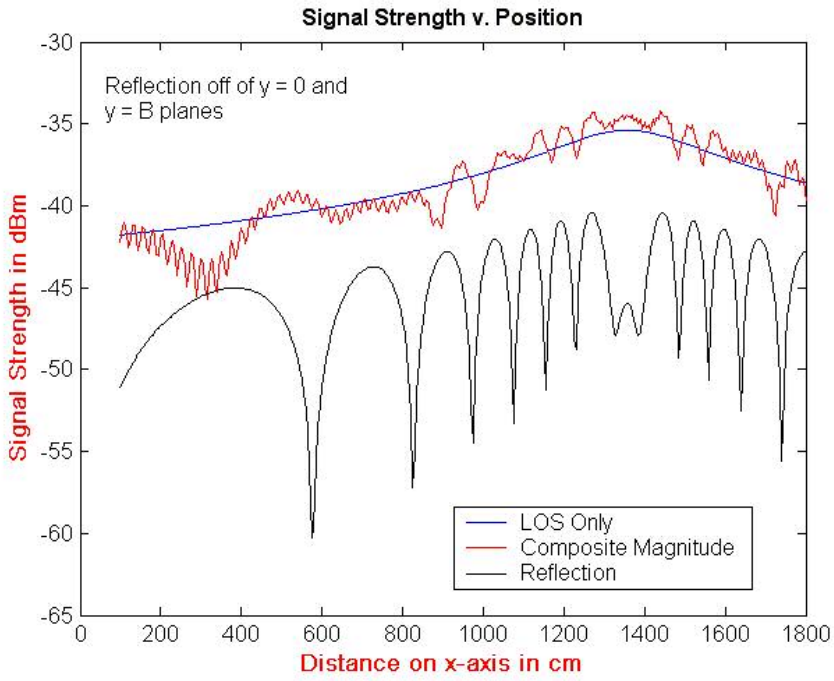

Fig. 6.5(a) Constituent Signals

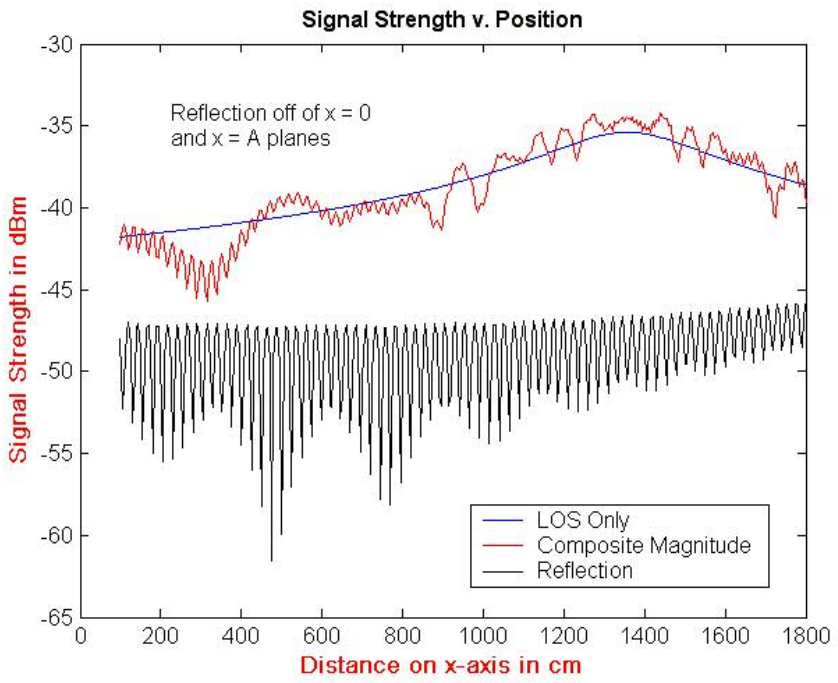

Fig. 6.5(b) Constituent Signals

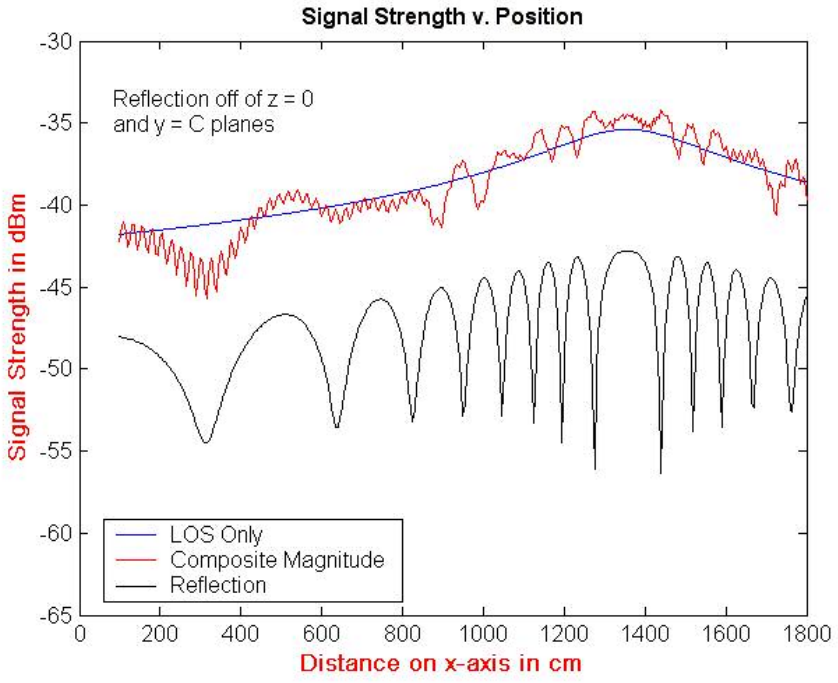

Fig. 6.5(c) Constituent Signals

In all cases, the reflection signal strengths (due to one pair of reflections) are lower than the LoS magnitude. This is due to absorption losses at the point of reflection as well as the increased distance traveled by the wave. Clearly the components are complex numbers and have to be added up resulting in the composites as shown in the figures indicating a considerable interference amongst the different rays. The composite signal always shows the most variation across the graph.

Note that using the model we can examine the contributions of each of the seven components of the composite signal. However, what is seen by any receiver is the composite signal only.

6.2 Contour Graphs

I look at some contour graphs to gain a better understanding of the situation. I look at a y-z plane parallel to the plane of the APs in Fig. 6.6. x is held at 500 cm, and the y, z coordinates are varied across their entire range. As before, the AP is at (1357, 180, 230).

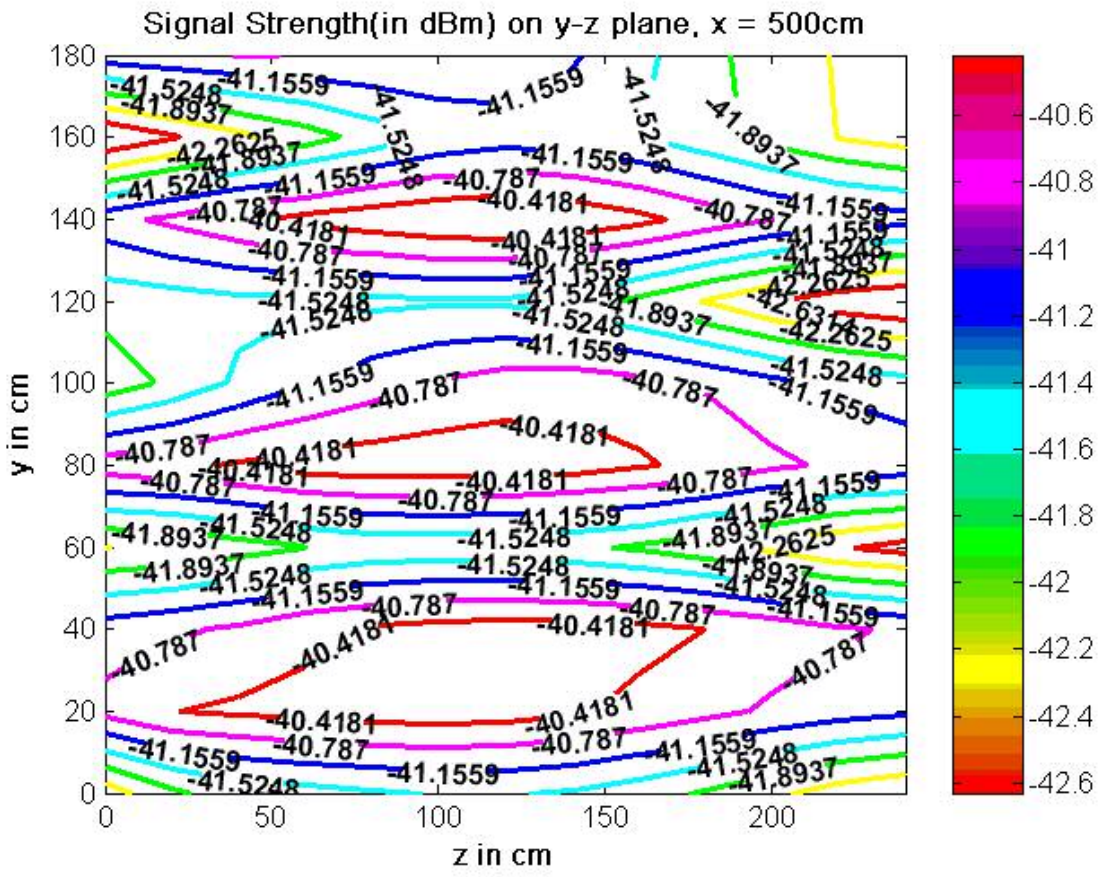

Fig. 6.6 Contour graph on y-z plane

There is a total variation of about 3 dBm across the plane. The distribution is due to the geometry of the situation.

I look at a y-z plane which is closer to the AP, with x = 1300(Fig. 6.7).

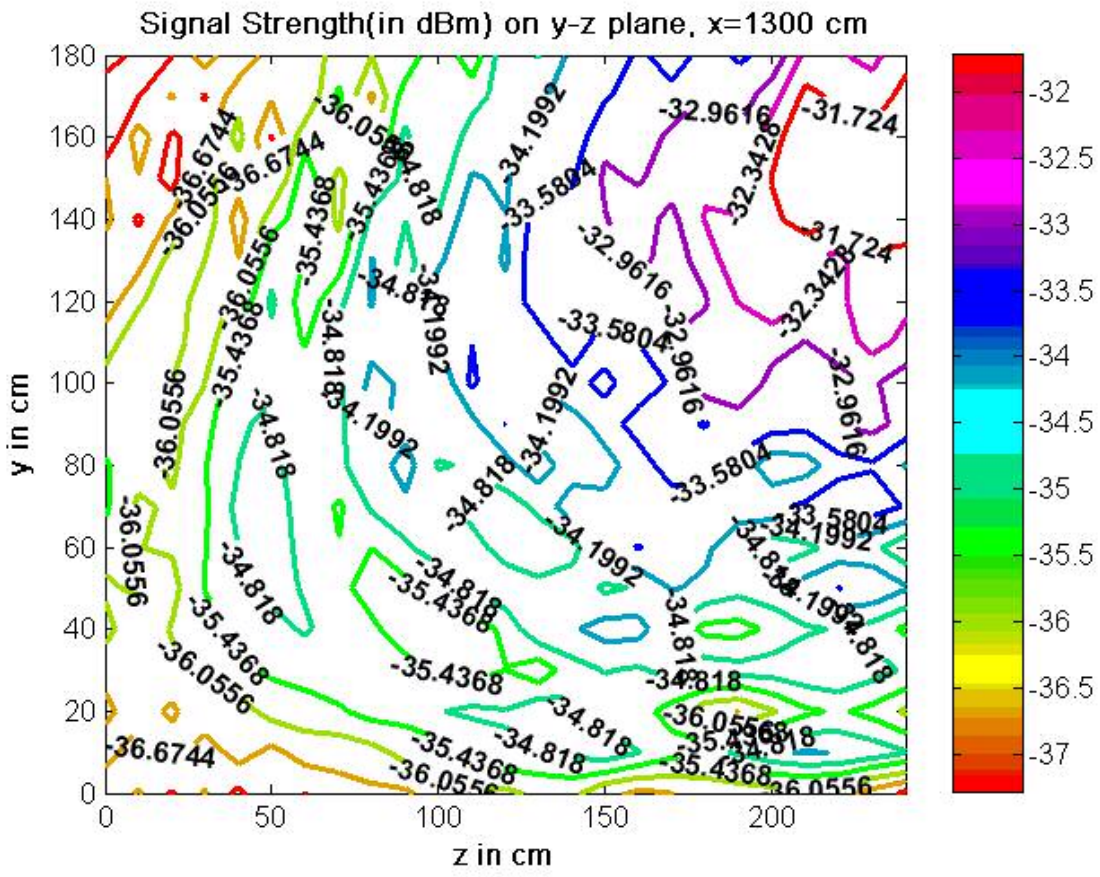

Fig. 6.7 Contour graph on y-z plane

The curves swirl towards the upper right corner, with successively higher signal strengths. This is because the AP is located in that region. There is a total variation of 6 dBm across the plane.

I look at a variation (Fig. 6.8) across the x-y plane(x is varied from 300 to 1600 cm, y from 0 to 185 cm), z is held constant at 92 cm. (This corresponds to values used in Expt. 2).

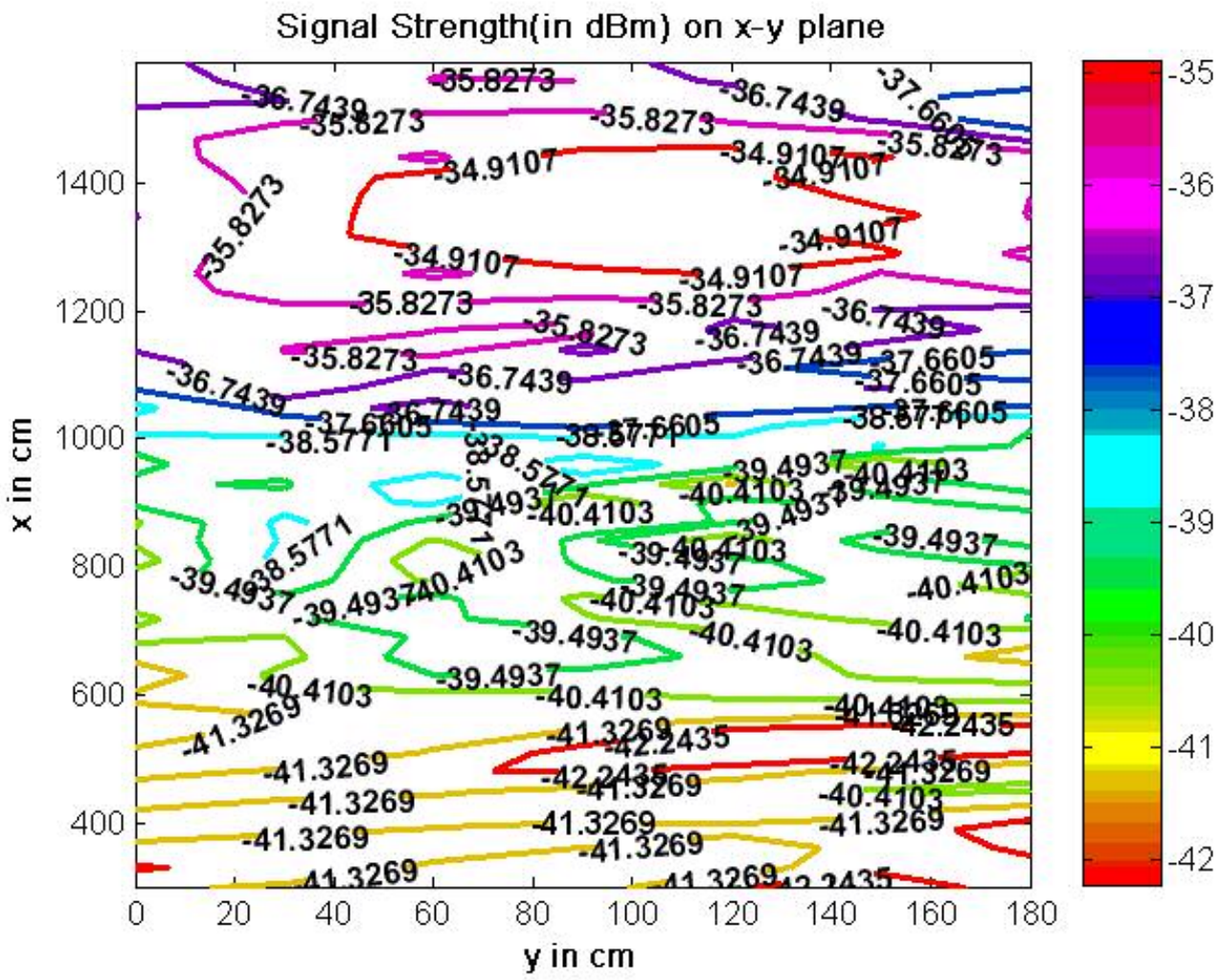

Fig. 6.8 Contour graph on x-y plane

Signal strengths increase with proximity to the AP, as in the experiment. There is a variation of 7 dBm across the plane.

Contour graphs are a useful tool in visualizing signal strength configurations in a given environment. Further, they can be used to predict the presence of ‘dead spots’ or regions of very low or non-appreciable signal strengths.

Chapter 7. Obstructions

The signal strength configuration changes in the presence of an obstruction in the path of the waves. Obstructions can include walls, ceilings, humans (possibly moving), and so on. Thus, studying this gives us better estimates of signal strength configurations. Further, an interesting application can be the prediction of the presence of obstructions (and their locations) by the measurement of signal strengths.

7.1 Theory and Models

Rays passing through an obstruction are attenuated [15]. (Note that this applies to rays in their LoS path between the transmitter and receiver, as well as to reflected rays.) The amount of absorption depends on the dielectric properties of the material. There are also diffraction and refraction effects which alter the signal strength configuration, but I will not consider that for now.

I modify my model to check if the rays from **T** to **R** fall within the coordinates of the obstruction. In those cases, eqn. 4.4.1 is modified as

$$J(x) = J_0 \gamma . x^{-D} e^{(\frac{2\pi f x}{c})} \qquad (7.1.1)$$

where γ is the transmission coefficient, the fraction of the magnitude transmitted through the material.

An attenuated signal configuration is expected in the presence of an obstruction. I plot some graphs to explore this.

First, I take a particular configuration, and plot signal strengths in the absence of (Fig. 7.1), and in the presence of(Fig. 7.2), an obstruction. The obstruction is set to have a transmission coefficient of 0.1.

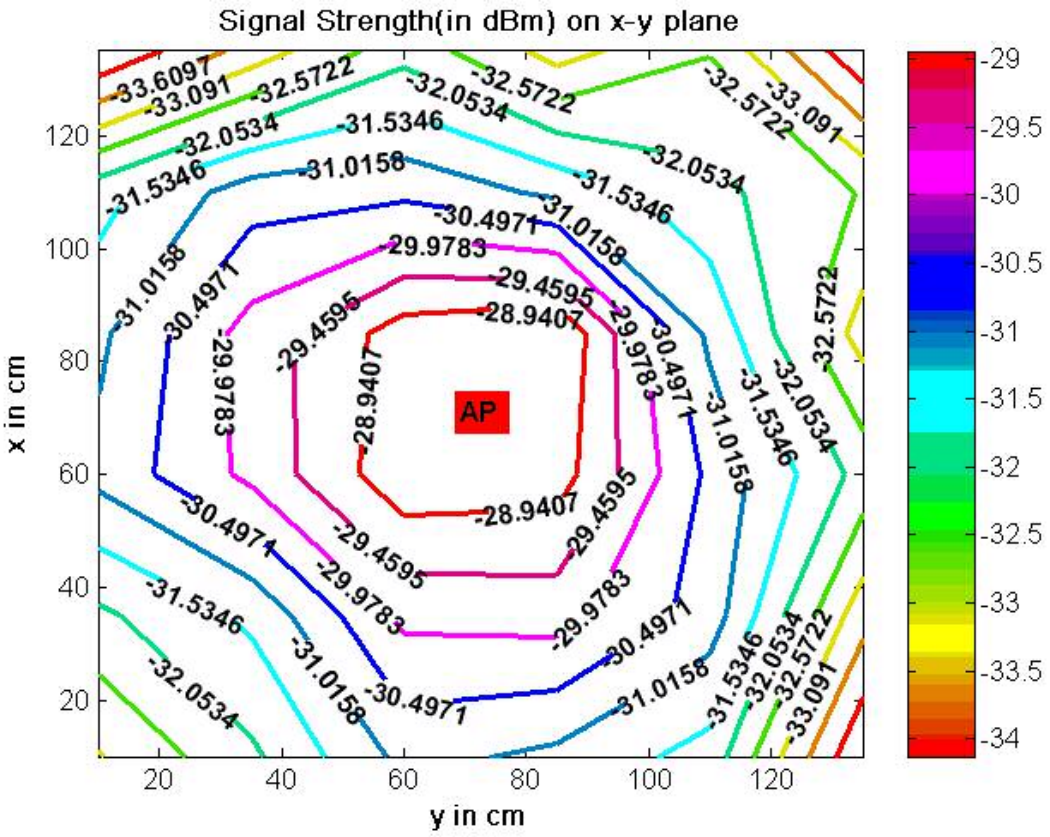

Fig. 7.1 Signal strength configuration with no obstruction

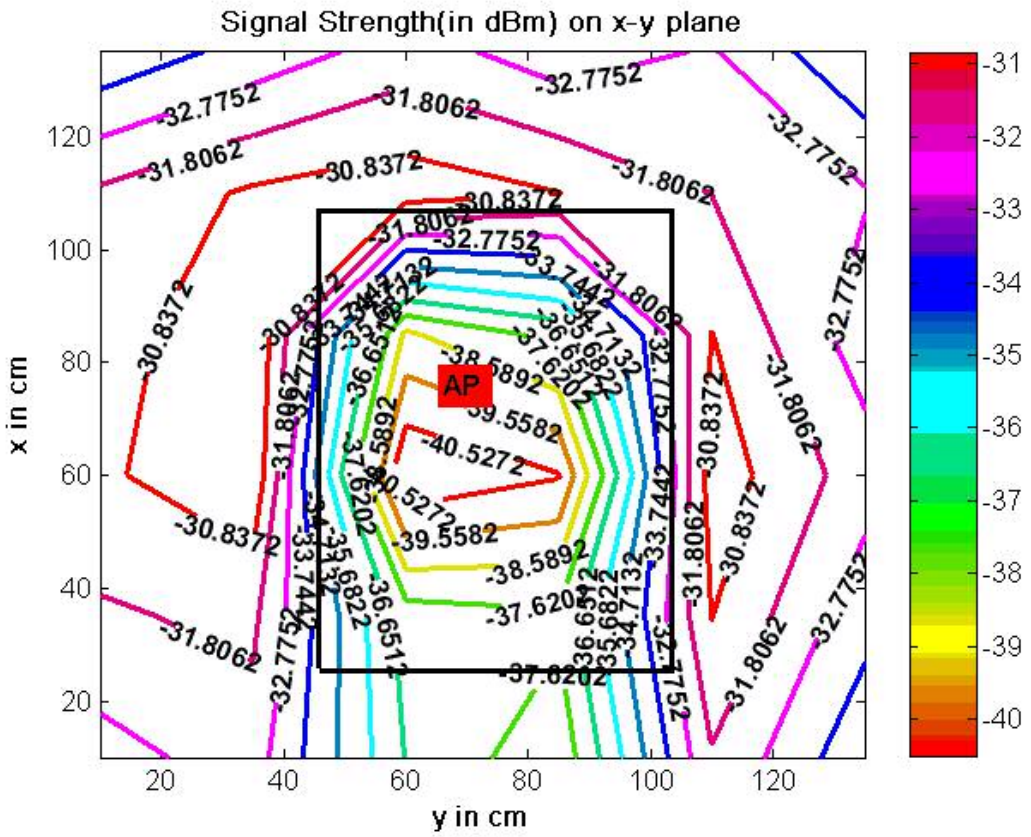

Fig. 7.2 Signal strength configuration with obstruction

It is seen that there is signal strength attenuation in Fig. 7.2 as compared to Fig. 7.1.

I move the obstruction closer to the AP in the model to get Fig. 7.3.

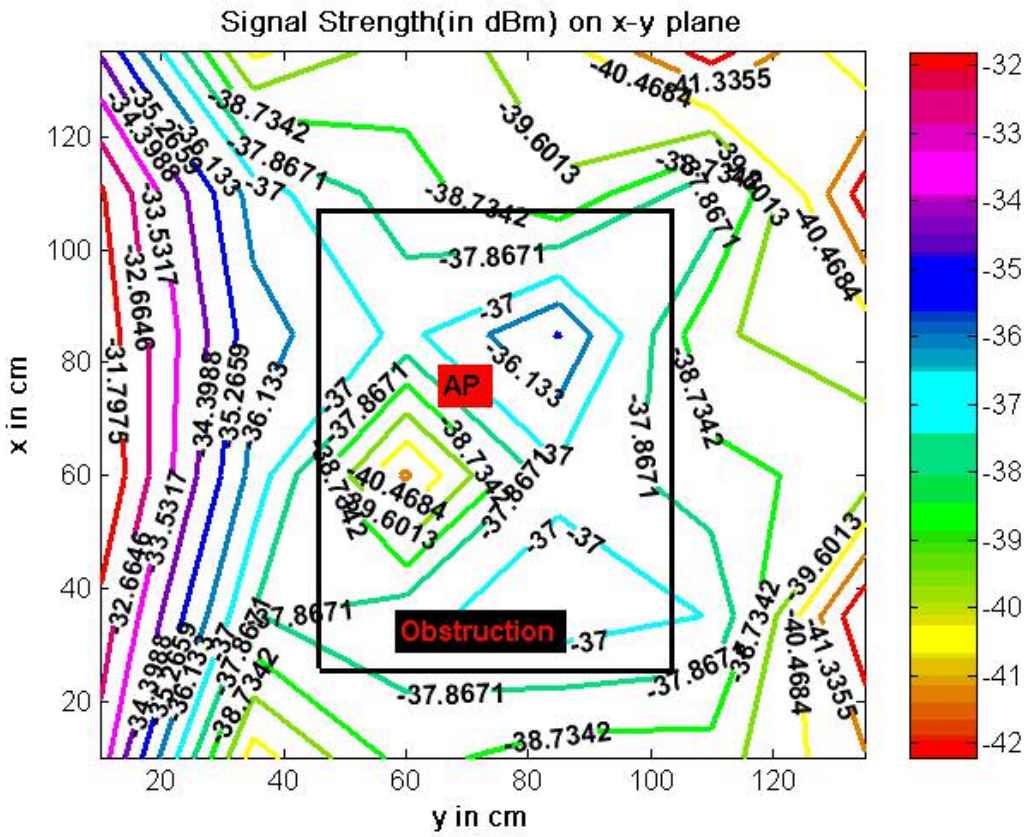

Fig. 7.3 Signal strength configuration with obstruction

For Fig. 7.4, I move the AP along the y-axis (in the model.)

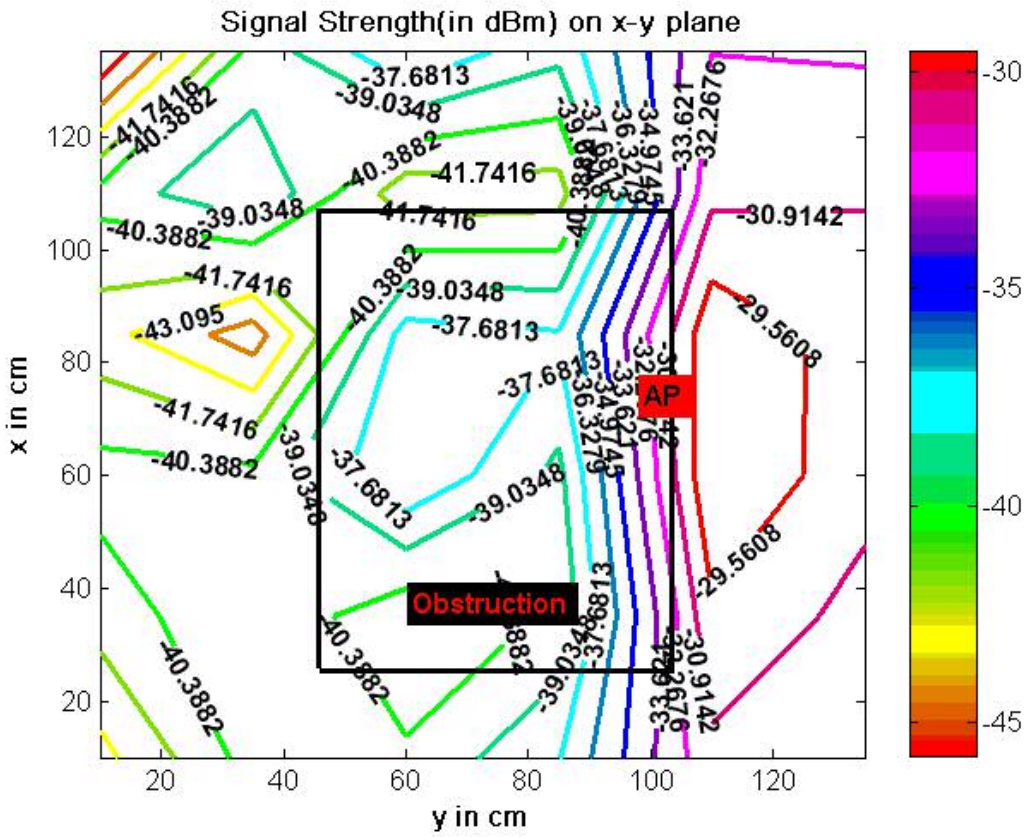

Fig. 7.4 Signal strength configuration with obstruction

The various non-symmetrical effects observed are because of the interference of the LoS and reflected rays.

7.2 Conclusions

There are very specific signal strength configurations that result depending on the presence and position of an obstruction. My model can be modified to include this effect to predict the resulting configuration with a good degree of accuracy.

Chapter 8. Concluding Remarks and Future Work

In this study I developed an analytic model for determining the signal strength at various locations in a 3-D rectangular space containing one Access Point. In my model I used the standard wave propagation equation and took into account multipath effects due to reflected waves received from six sides of the rectangular box. My measurements, conducted to verify the model, indicate that the model with single reflections shows sufficient accuracy and can be used effectively.

Using the model, I calculated signal strengths along several axes and on several planes. All of these calculations show significant variability in the signal strength. Of note is the fact that the signal strength can change by several dBms as the location changes by a few cms. Such changes in the signal strength may not have any serious consequences for data transmission. However, when the signal strength measurements are used for other purposes, such as determining the location, the consequences of such variability can be very far reaching. Also, as most WiFi systems use the signal strength to decide which AP to associate with, a significant change in the measured signal strength can trigger a handover where one may not be necessary.

I looked at models of signal strength attenuation in the presence of an obstruction in the path of the RF waves. These results indicate that the changes in the signal strength depend significantly on the location and type of the obstruction. This knowledge can be used for determining the location of an obstruction, such as a person, in the corridor.

The work presented in this thesis is the first step in developing detailed and workable analytic models for indoor space. Many additional practical details will have to be included in the enhanced models. This work can be extended in several directions. For example the model can be enhanced to:

- Include other effects such as refraction, scattering, and fading.
- Incorporate more detailed effects due to people walking by, and other obstructions in the room.
- Study how the signal strength changes while an obstruction moves through the room.
- Study the effects of multiple reflections.
- Include effects due to the characteristics of the AP. I have made an approximation of the AP as a fixed point, radiating rays uniformly in all directions. This is not true in real life, but depends on the specific antenna involved. The distribution pattern of the antenna can also be reflected in the model.
- Study in greater detail the causes of discrepancies between the model and experiment.

References

(1) "**Modern Approaches in Modeling of Mobile Radio Systems Propagation Environment"**, *IEEE* Communications Surveys and Tutorials: *Aleksandar Neskovic, Natasa Neskovic, and George Paunovic, University of Belgrade*

(2) "**Short Distance Attenuation Measurements at 900MHz and 1.8GHz Using Low Antenna Heights for Microcells"**, *IEEE JSAC*, vol. 7, no. 1, Jan. 1989: *P. Harley*

(3) "**Radio Propagation Characteristics for Line-of-Sight Microcellular and Personal Communication**", *IEEE Trans. Ant. and Prop.*, vol. 41, no. 10, Oct. 1993.: *H. H. Xia et al.*

(4) "**Artificial Neural Network Indoor Radio Propagation Model (band 900MHz)",** Master's Thesis, Faculty of Electrical Engineering -- Belgrade, 1997: *A. Neskovic*

(5) "**Short Distance Attenuation Measurements at 900MHz and 1.8GHz Using Low Antenna Heights for Microcells**", *IEEE JSAC*, vol. 7, no. 1, Jan. 1989.: *P. Harley*

(6) "**Finite Conductivity Uniform GTD Versus Knife-edge Diffraction in Prediction of Propagation Path Loss**," *IEEE Trans. Ant. Prop.,* vol. AP-32, Jan. 1984: *R. J. Luebbers*

(7) *"***Wireless Information Networks**", New York: John Wiley & Sons, Inc., 1995: *K. Pahlavan and A. H. Levesque*

(8) "**Indoor Electric Field Level Prediction Model Based on the Artificial Neural Networks**," *IEEE COMML*, vol. 4, no. 6, June 2000 : *A. Neskovic, N. Neskovic, D. Paunovic*

(9) "**Influence of the Human Body on Indoor Radio Communications at 450MHz -- Measurements and Analysis**", *Proc. 43th Annual Conf. ETRAN*, Budva -- Yugoslavia, June 1996: *A. Neskovic, N. Neskovic, and D. Paunovic*

(10) "**Indoor geolocation science and technology**", *Communications Magazine*, IEEE , Volume: 40 , Issue: 2 , Feb. 2002:*K. Pahlavan, Li Xinrong, J.P. Makela*

(11) " **Radio propagation modeling for indoor geolocation applications**", *Personal, Indoor and Mobile Radio Communications,* 1998. The Ninth IEEE International Symposium on , Volume: 1 , 8-11 Sept. 1998 : *P. Krishnamurthy, K. Pahlavan, J. Beneat*

(12) "**Wideband radio propagation modeling for indoor geolocation applications**", *Communications Magazine*, IEEE , Volume: 36 , Issue: April 4, 1998 : , *K. Pahlavan, P. Krishnamurthy, A. Beneat*

(13) "**A comparison of wireless geolocation algorithms in the indoor environment**", *Wireless Communications and Networking Conference*, 2004. WCNC. 2004 IEEE , Volume: 1 , 21-25 March 2004: *K. Pahlavan, M. Kanaan*

(14) **'Radio propagation models'** : 'http://people.deas.harvard.edu/~jones/es151/prop_models/propagation.html #harley'

(15) **' Wireless Communications — Principles and Practice'**: *Theodore S. Rappaport*

(16) '**Indoor Radio Channel Propagation Modelling by Ray Tracing Techniques**', PhD Thesis: *David I. Laurenson*

(17) '**Radio Propagation in Cellular Networks'**, *N. Blaunstein*

(18) '**Physics, Part I'**, Resnick and Halliday